Fibers and Polymers 2013, Vol.14, No.2, 298-303 DOI 10.1007/s12221-013-0298-x

Multifunctional Melt-Mixed Ag/TiO$_2$ Nanocomposite PP Fabrics: Water Vapour Permeability, UV Resistance, UV Protection and Wear Properties

Roya Dastjerdi* **and M. R. M. Mojtahedi**[1]

Textile Engineering Department, Yazd University, Yazd, Iran
[1]*Textile Engineering Department, Center of Excellence in Textile, Amirkabir University of Technology (Tehran Polytechnic), Tehran, Iran*

(Received March 10, 2012; Revised June 28, 2012; Accepted July 25, 2012)

Abstract: This research deals with the investigating the effect of nanoparticles on the various properties of nanocomposite fabrics produced from melt spinning of various blend ratios of prepared masterbatch containing Ag/TiO$_2$ nanoparticles. The results revealed that the wear properties of modified fabrics improved as compared to pure fabrics with a trend justified considering modulus or crystallinity of fabrics with opposite effects. About 40 % UV protection enhancement has been obtained applying this kind of nanoparticles in the close relationship with the crimp contraction of textured yarns. A considerable improvement in the garment comfort has been recorded for nanocomposite sample containing 1 wt% nanoparticles. The lower permeability at low environment temperature and a higher at higher one, as compared to the pure sample, were obtained using this sample. It is highly interesting that these desirable changes in permeability can be achieved in the range of common environment temperatures (15-35 °C) being adapted to the human body requirements. The changing point is about 25 °C exactly meeting the body requirements by changing environment temperatures. A UV-induced solid state nanocomposite interaction increasing wear properties of UV-irradiated nanocomposite fabrics has been discovered.

Keywords: Masterbatch, UV-induced solid state nanocomposite interaction, Fabric comfort, Melt spinning, Abrasion resistance

Introduction

Polypropylene fibers are one of the most widely used synthetic fibers in textile industry especially considering their various application fields. In fact, some advantages of this fiber type, including cheapness, lightness and high chemical strength have made it suitable for many demands such as carpets, automotive interior trim, films, packaging, cover stock, cables, napkins, wipes, and so on [1]. However, PP applications are limited because of its low UV. resistance [2]. In addition, one of the weak spots of knitted fabrics is their low abrasion resistance. Relatively low vapor permeability also limits the comfort of PP fabrics. Consequently, this paper has focused on the investigation of wear properties, UV resistance, water vapor permeability and UV protection properties of melt mixed PP knitted nanocomposite fabrics.

Film and fiber processing are the most difficult polymeric molding procedures. Most of the works on producing PP nanocomposite yarns have been limited to low speed spinning, with laboratory machine and/or producing thick monofilament as spun yarns. Toshniwal *et al.* [3] have produced clay/PP yarns with the take up speed of 31 m/min and evaluated their dyeability. Razamahefa *et al.* [4] have investigated the dyeing properties of clay/PP nanocomposite yarn produced with the low speed spinning and final linear density of 2000 dtex. Pavlikova *et al*. [5] have investigated rheological and morphological properties as well as tensile strength of clay/PP nanocomposite yarns produced with the take up speed of 150 m/min. Producing monofilament of bicomponent PP/Ag nanocomposite as-spun yarns and investigating their morphological and antibacterial properties have been reported by Yeo *et al.* [6]. Erdem *et al.* [7] have reported the UV. protection properties of produced TiO$_2$ nanocomposite yarns. However, measuring the UV. protection over yarns cannot be sufficiently accurate. Therefore, producing fabric can provide more suitable conditions. With respect to the fact that producing nanocomposite multifilament yarns via a pilot plant or an industrial process is required for preparing the fabrics [8], the effect of nanoparticles on the mentioned properties of fabrics made of fine nanocomposite multifilament yarns has not been reported in the literature as far as we concern. Therefore, investigating the aforementioned properties of melt mixed nanocomposite fabrics made of continuous fine multifilament nanocomposite yarns has been conducted in this article as a novel research.

Experimental

Materials and Methods

In fact, this research has been started from the modification of polymer powder as a by-product of petrochemical companies [9]. The fabric has been produced in our previous research [9] briefly as follows: Polypropylene (iPP) powder and the Ag/TiO$_2$ nanocomposite powder were premixed and melt blended in a co-rotating screw extruder (Brabender, Germany) for masterbatch preparation. Pure PP fibers and the nanocomposite fibers containing 0.20, 0.35, 0.50, 0.75, 1.00 wt% of silver/TiO$_2$ nanocomposite were prepared

---

*Corresponding author: nanobiotex@yahoo.com

Table 1. Introducing of produced samples

Sample code	Weight percentage of nanoparticles (Ag/TiO_2)
NP0	0.00
NP0.20	0.20
NP0.35	0.35
NP0.5	0.50
NP0.75	0.75
NP1	1.00

during melt spinning by an Automatik pilot plant spinning machine (Germany) from mixing of virgin PP granule and concentrated master-batch containing 20 wt% Ag/TiO_2 nanoparticles. All the prepared samples are introduced in Table 1. The drawn samples have been prepared with a Zinser D5203 drawing machine (Germany). The variable draw ratio was used to gain the constant breaking elongation of 50 %. The above breaking elongation was selected to be suitable for further texturing. A Scragg-Shirley minibulk false-twist texturing machine (England) was employed with the heater temperature of 150 °C, draw ratio of 1.07, texturing speed of 100 $m \cdot min^{-1}$ and applied twist of 2953 tpm. A full characterization of as-spun, drawn and textured yarns (including morphological properties (SEM), density-based crystallinity, thermal analysis ((DSC), linear density, tensile and mechanical properties, shrinkage, crimp properties, etc. has been reported, in parallel with their bioactivity, in our previous paper [9]. A three-ply textured yarn, made of the three textured bobbin yarns, of each full-defined sample was finally weft knitted on a single circular knitting machine operating 120 needles with 8.9 cm (3.5 inch) diameter to prepare each fabric sample.

Characterization

A martindale abrasion tester machine was employed to measure the resistance of fabric samples to abrasion, according to ASTM D4966. Water vapor permeability (WVP) of prepared pure and nanocomposite fabrics evaluated according to ASTM (E 96-80B) [10].

Evaluating the color changes of wool fabrics dyed by a highly UV sensitive dye (0.5 % (owf) Methylene Blue) supported by pure and nanocomposite produced fabrics under UV irradiation was considered to compare the UV protection properties of samples [11,12]. The dying of wool fabrics was performed in the dye baths including 0.5 % (owf) the Methylene Blue using a 40:1 liquor ratio. The fabrics were immersed for 10 mins at the environment tempratuer. Dyeing was performed by raising the temperature of the dye bath to 85 °C at the rate of 2.5 °C/min, and holding at this temperature for 30 mins and then cooling the bath to 60 °C at the rate of 2 °C/min. The dyed fabrics were, then, 4 times rinsed in distilled water and dried at the environment temperature. UVC irradiations were provided by UVC lamp (G30T8 TUV3 foot 30W germicidal UVC30) located 10 cm above the covered samples for 8 h. After UV irradiation the color changes were studied based on reflectance data using a Color Eye7000A Spectrophotometer. $\Delta E\%$ was calculated according to equation (1).

$$\Delta E(\%) = [(\Delta E_p - \Delta E_C)/\Delta E_p] \times 100 \tag{1}$$

ΔE_p and ΔE_C are color differences of each wool fabric supported by pure and composite samples, respectively which are calculated according to equation (2).

$$\Delta E_{PorC} = [(L_0 - L_{PorC})^2 + (a_0 - a_{PorC})^2 + (b_0 - b_{PorC})^2]^{0.5} \tag{2}$$

Where L, a and b are the values of lightness, redness–greenness, and yellowness-blueness, respectively determined using computer color matching system. L_0, a_0 and b_0 refer to dyed wool fabrics before UV irradiations [12]. The Wear resistance properties of fabric samples after 16 and 64 h UV irradiation with UVC lamp (G30T8 TUV3 foot 30W germicidal UVC30) located 10 cm above the samples have been considered as the criteria of UV. resistance of different samples and measured according to the ASTM D4966. The average value of triplicate tests of each aforementioned experiment has been reported. The percentage of changing the crimp contractions (CC%) as compared to pure sample has been considered for some discussions. The crimp properties of textured yarns were measured after the heating period of 10 min at 120 °C according to the DIN 53840 using the following equation.

$$CC\% = \frac{L_g - L_z}{L_g} \times 100 \tag{3}$$

Briefly, L_g has been evaluated as the hank length of reeled yarn after loading of 2 cN/dtex for 10 s. L_Z is the hank length of the reeled yarn after diminishing of the load to 0.01 cN/dtex for 10 mins. The average of five measurements for each sample has been reported in our previous paper [9].

Results and Discussion

Wear Properties

Weight reduction of samples during the abrasion test has been recorded in Figure 1. The slope of the weight reduction and the number of rubs at the breaking point can be extracted from this figure. These two factors are the desirable criteria for the evaluation of fabric wear resistances. The slope of the weight reduction for each sample equaled the first derivative of weight reduction has been indicated in Figure 1. The number of rubs at the breaking point has been also reported for each sample in Table 2.

The results revealed that nano-filler improved the wear properties of the modified fabrics as compared to the pure

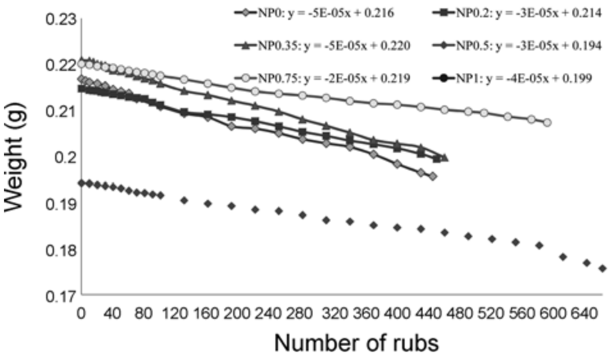

Figure 1. The weight reduction versus number of rubs.

fabric. The effect of nanostructured materials on the enhancement of nanocomposite wear resistance has been justified by the improvement of either mechanical or chemical properties [13].

In fact, the enhancement of modulus and hardness, or an improvement in bonding between filler and metallic counterparts can cause an enhancement in abrasion resistance of nanocomposites [13].

In this research, the trend of wear resistance was completely in agreement with the modulus trend of textured yarns [9]. However, the sample containing 0.75 nanoparticles has demonstrated a different trend in weight reduction slope in Figure 1. This phenomenon can be justified with minimum crystallinity in this sample [9] resulted in the enhancement of flexibility and work of rupture, as previously reported [9], causing lower rate of weight reduction for this sample.

The other factor that can affect the fabric abrasion resistance of nanocomposite fabric is thermal transfer acceleration resulted by high thermal conductivity of silver nano-particles. In fact, the friction between abradant and sample fabric during testing, generates a significant heat for the fabric subjected to wear test. Silver nanoparticles have a high thermal conductivity as compared to polypropylene as a non-polar polymeric matrix. Therefore, these particles can compensate the impact effect of this thermal generation and cause fabric destroying to be delayed. However, increasing the fraction of nanoparticles may result in some agglomeration which possibly declines the effect of particles on heat transfer rate because of leading to the decrease of the specific surface of the particles. Agglomeration can also decrease the wear resistance because of generating more discontinuities in the substrate.

Another reason that can be considered for the improvement of wear properties of nanocomposite fabrics is the mechanism of energy dissipation via voiding, dewetting phenomena, chain slippage [14], the steric hindrance of particles against the rotation or movement of polymer chains [15] and increasing the length of crack path (zig-zag route) in polymer/filler composite [14] which is related to the mechanism of modulus and tenacity enhancement in polymeric nanocomposites.

UV Irradiation Stability

The abrasion resistance of fabrics after UV irradiation has been studied as a criterion of structural stability of PP fabrics against UV irradiation. Figure 2 shows the abrasion resistance behavior of pure and nanocomposite yarns after 16 h UV irradiation. Weight reduction of samples during the abrasion test is recorded in this figure. The slope of the weight reduction for each sample has been indicated in Figure 2. The number of rubs at the end point (broken point) has been reported in Table 2. Although the UV irradiation reduced the broken point and abrasion properties of pure pp, the recorded broken point for nanocomposites were even more than their value before UV. irradiation. This phenomenon means the forming of new interactions between polymeric matrix and Ag/TiO_2 nanoparticles. Carbonyl, hydroxyl and/or hydroperoxide groups generated by the initiation of UV degradation of PP [2] can provide these interactions schematically demonstrated in Figure 3. Interestingly it has been increased by adding nano-particles ratio in sample containing 0.75 % NPs with the least crystallinty [9]. In fact, in this sample, most of the particles have located in the amorphous regions and consequently they can connect to the reactive radicals generated by the initiation of UV degradation of PP [2] in the amorphous regions. Therefore, the most enhancement has been observed for this sample. However, agglomeration of nanoparticles as confirmed by SEM micrographs [9] and the steric hindrance limited the efficient interaction by adding a more ratio of nano-particles. Consequently, crystallinty and steric hindrance are key factors for this UV induced solid state interactions increasing wear properties of the nanocomposite. As we know, this UV

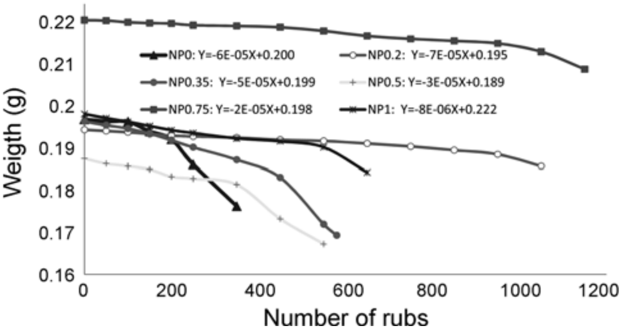

Figure 2. The weight reduction versus number of rubs after 16 h UV. irradiation.

Table 2. Number of rub at the breaking point

Irradation time (h)	0	16	64
NP0	445	350	40
NP0.20	450	1050	80
NP0.35	460	580	100
NP0.5	660	550	130
NP0.75	580	1150	110
NP1	640	650	160

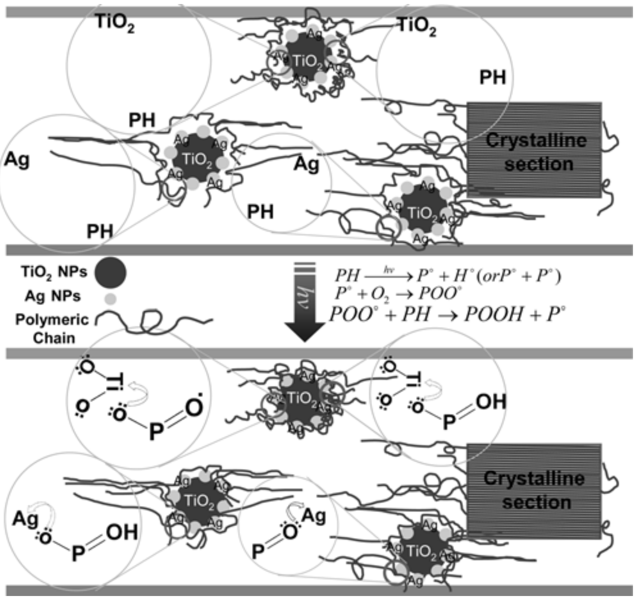

Figure 3. Schematic of the UV induced solid state interactions in the polymeric nanocomposites.

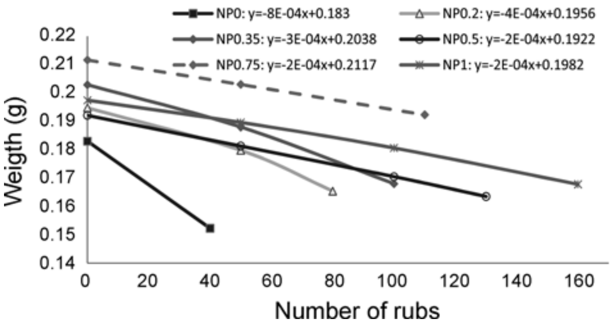

Figure 4. The weight reduction versus number of rubs after 64 h UV. irradiation.

induced solid state interaction has been discovered in this research for the first time and has not been reported so far. However, increasing the UV irradiation time resulted in appearing the degradation phenomena for all samples. Figure 4 shows the abrasion behavior of samples after 64 h of UV irradiation. Although the degradation phenomena can be seen for all samples, the resistance and wear properties of nanocomposite samples are still considerably more than the pure samples. The broken point recorded for the irradiated nanocomposite samples is 4 times greater than the pure sample which means 300 % improvement of abrasion resistance for the UV. irradiated PP nanocomposites as compared to UV. irradiated pure PP. The rate of weight reduction of pure samples changed from 8×10^{-3} for the pure sample to 2×10^{-3} for samples containing 0.5, 0.75 and 1 wt% nanoparticles. Consequently, the rate of weight reduction of pure sample is 4 times faster than nanocomposites.

UV Protection Properties

In parallel with public concern about the serious and chronic side effects of sunlight exposure, such as sunburn, malignant melanoma and skin cancer, investigations to control these side effects are increasingly carried out. Garments act as an important support to prevent this hazardous sunlight [16-19]. Using nanocomposites is a remarkable modification method. Among inorganic nanoparticles titanium dioxide (TiO_2) is a well-known semiconductor photocatalyst with unique properties (e.g. stable, long lasting, secure and broad spectrum). It is widely used in sunscreen lotions as active broadband sunscreen [20]. Silver can improve the photocatalytic activity of TiO_2 [21,22]. In fact, Ag can act as the electron traps aiding electron-hole separation, and also facilitates electron excitation by creating a local electric field [22]. Moreover, TiO_2 [23-31] and silver [32-37] are the safest and the most used inorganic nanostructures for modification of polymeric materials and are attracted to develop multifunctional nanocomposites [38]. Figure 5 shows the enhanced UV. protection properties as compared to pure fabrics. About 30-40 % improvement of UV. protection properties has been recorded for nanocomposite samples. A close relationship between the trend of promotion effect of nanoparticles and crimp contraction of textured yarns can be found. By adding 0.2 wt% nanoparticles, an improvement of more than 30 % in UV protection properties has been recorded. In parallel with increasing the nanoparticle content and decreasing the crystallinity [9], the maximum promotion effect (about 40 %) has been recorded for nanocomposite fabrics containing 0.35 wt% nanoparticles. In fact, blocking particles in the crystalline part can limit their incorporation to absorb UV irradiation. Therefore, reduction of the crystallinity showed a positive effect in this sample. However, the most important role was played by crimp contraction. This can be concluded through considering the changes of crimp contraction [9] of nanocomposites as compared to pure yarns reported in Table 3. The intensity of the promotion effect decreased in the sample containing 0.5 wt% nanoparticles to some extent. Nevertheless, by increasing the nanoparticle content, the

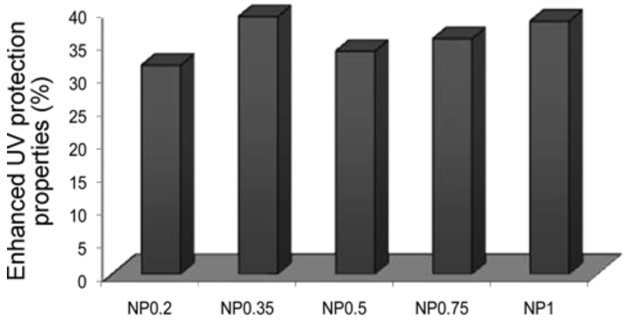

Figure 5. The percentage of enhanced UV protection properties of nanocomposites as compared to pure samples.

Table 3. The percentage of changing the crimp contractions (CC%) as compared to the pure sample [9]

Sample code	CC% changes
NP0	0
NP0.20	4.73
NP0.35	-3.30
NP0.5	-12.04
NP0.75	-7.60
NP1	-6.09

changes have been compensated and are not significant. However, increasing the promotion effect was limited by agglomeration decreasing the special surface area of nanoparticles in the sample containing more nanoparticle ratios. Therefore, the maximum recorded enhancement was about 40 % as compared to pure sample.

Water Vapour Permeability

The water vapor permeability of pure and nanocomposite samples after 4 hr. versus environment temperature has been exhibited in Figure 6. As shown in this Figure, at high environment temperatures the maximum permeability has been recorded for nanocomposite sample containing 1 wt% nanoparticles. Figure 7 shows the percentage changes of permeability of nanocomposite sample containing 1 wt% masterbatch at different temperatures. This sample demonstrated 11.2 % permeability improvement as compared to pure sample at 30 °C.

Increasing the permeability at temperatures above 25 °C simplifies removing the body heat as well as sweat and consequently offers more comfort for garment, tent, curtain etc. By decreasing the temperature, permeability decreased for both pure and the nanocomposite samples. It is interesting to mention that the rate of permeability decline is sharper for the nanocomposite sample and this sample has less permeability than the pure sample at all temperatures below 25 °C. This sample shows about 10.33 % permeability decline at 15 °C. This lower vapor permeability at low temperature protects the body from cool weather through preventing loss of body heat and weather flow. The lower permeability at low temperature and the higher at higher one can be obtained using this sample. According to statistical analyses, the differences between pure PP and nanocomposite containing 1 wt% nanoparticles were statistically significant in all temperatures except 25 °C. It is highly interesting to notice that these desirable changes in permeability have been achieved in the range of common environment temperatures (15-35 °C) being adapted to the human body requirements. The changing point is about 25 °C, exactly meeting the body requirement by changing environment temperatures, which is really a worthwhile achievement. Consequently this nanocomposite sample can provide more comfortable textile for different applications such as garment, tent, etc.

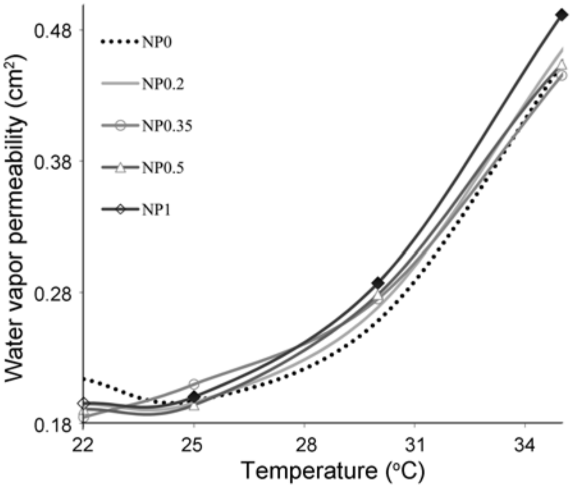

Figure 6. The water vapor permeability of pure and nanocomposite samples versus environment temperatures.

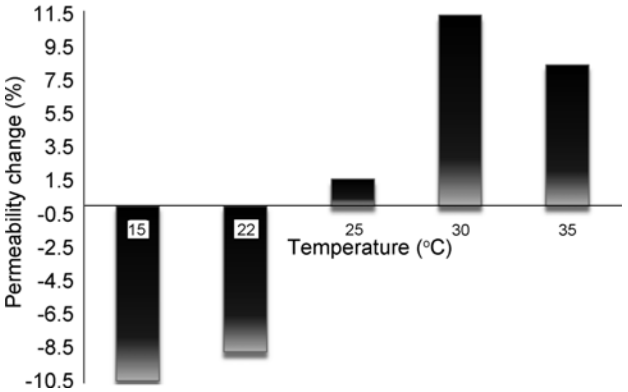

Figure 7. The percentage changes of permeability of nanocomposite sample containing 1 wt% nanoparticles (NP1) as compared to pure PET fabrics (NP0) at different environment temperatures.

Inorganic nanoparticles are impermeable materials. At a low temperature nanoparticles may act as a barrier and prevent permeability. Nanoparticles can also limit the movement of polymeric chain because of steric hindrance of particles against chain motion [12]. Increasing kinetic energy at a high temperature can compensate this effect. Therefore at a high temperature decreasing crystallinity caused by nanoparticles can be effective as a key factor which leads to the increase of the amorphous regions and hence the permeability. However, changes in yarn such as linear density, crimp contraction, etc., and thus fabric structures such as cover factor can also be effective. The associated effect of all mentioned factors led to this improvement of permeability for sample containing 1 wt% masterbatch. This nanocomposite fabric can smartly adapt permeability with human body requirement by changing the environment temperatures.

Conclusion

This paper deals with investigating the effect of the nanoparticles on the various properties of nanocomposite fabrics. For this goal, prepared fabrics made of Ag/TiO_2/PP nanocomposite multifilament yarns have been subjected to the standard abrasion resistance test, as well as water vapour permeability, UV resistance and UV protection tests. These fabrics have been produced in our previous research via melt mixing of inorganic nanoparticles and PP in a co-rotating screw extruder, masterbatch preparation, melt spinning, drawing, texturing and knitting [9]. The results disclosed a close relationship between the abrasion resistance and modulus or crystallinity of fabrics. These two factors had tow contradictory effects on the abrasion resistance. In fact abrasion resistance improved by the enhancement of modulus while decreasing of crystallinity. Nanoparticles improved the stability of fabric against UV degradation as a major weak point of PP. A UV induced solid state interaction has been realized by this research increasing wear properties of the nanocomposite. The results showed the increasing of the water vapor permeability at temperatures above 25 °C and decreasing permeability at all temperatures below 25 °C. This simplifies removing of body heat and sweat and consequently offers more comfort for garment, tent, curtain etc. at temperatures above 25 °C, while lower vapor permeability at a low temperature protects the body from cool weather through preventing loss of the body heat and weather flow.

References

1. R. Dastjerdi, M. R. M. Mojtahedi, A. M. Shoshtari, and A. Khosroshahi, *J. Text. Inst.*, **101**, 204 (2010).
2. S. Aslanzadeh and M. H. Kish, *Fiber. Polym.*, **11**, 710 (2010).
3. L. Toshniwal, Q. Fan, and S. C. Ugbolue, *J. Appl. Polym. Sci.*, **106**, 706 (2007).
4. L. Razamahefa, S. Chlebicki, I. Vroman, and E. Devaux, *Coloration Technology*, **124**, 86 (2008).
5. S. Pavliková, R. Thomann, P. Reichert, R. Mülhaupt, A. Marcinčin, and E. Borsig, *J. Appl. Polym. Sci.*, **89**, 604 (2003).
6. S. Y. Yeo, H. J. Lee, and S. H. Jeong, *J. Mater. Sci.*, **38**, 2143 (2003).
7. N. Erdem, U. H. Erdogan, A. A. Cireli, and N. Onar, *J. Appl. Polym. Sci.*, **115**, 152 (2010).
8. R. Dastjerdi, M. R. M. Mojtahedi, and N. Hidari, *J. Appl. Polym. Sci.*, **125**, 3688 (2012).
9. R. Dastjerdi, M. R. M. Mojtahedi, and A. M. Shoshtari, *Fiber. Polym.*, **9**, 727 (2008).
10. S. Mondal and J. L. Hu, *J. Appl. Polym. Sci.*, **103**, 3370 (2007).
11. L. Todorova and V. Vassileva, *Fibers Text. East. Eur.*, **11**, 21 (2003).
12. R. Dastjerdi, M. Montazer, and S. Shahsavan, *Colloid. Surface. B*, **81**, 32 (2010).
13. Z. Zhang, C. Breidt, L. Chang, F. Haupert, and K. Friedrich, *Compos. Part A-Appl. S.*, **35**, 1385 (2004).
14. K. G. Gatos, N. S. Sawanis, A. A. Apostolov, R. Thomann, and J. K. Kocsis, *Macromol. Mater. Eng.*, **289**, 1079 (2004).
15. R. Dastjerdi, M.sc. Dissertation, Amirkabir University of Technology, Tehran, 2006.
16. S. Yun and D. Schlossman, "Proceedings of the PCIA Conference", Shanghai, 1999.
17. W. D. Schindler and P. J. Hauser, "Chemical Finishing of Textiles", Woodhead Publishing, Cambridge, UK, 2005.
18. K. Hoffmann, K. Kaspar, T. Gambichler, and P. Altmeyer, *J. Am. Academy of Dermatol.*, **43**, 1009 (2000).
19. A. R. Scott, "Textile for UV Protection Part 13", The Textile Institute, Cambridge, England, 2005.
20. C. Contado and A. Pagnoni, *Anal. Chem.*, **80**, 7594 (2008).
21. R. Dastjerdi, M. R. M. Mojtahedi, and A. M. Shoshtari, *Macromol. Res.*, **17**, 378 (2009).
22. A. L. Linsebigler, G. Lu, and J. T. Yates, *Chem. Rev.*, **95**, 735 (1995).
23. R. Dastjerdi, M. Montazer, T. Stegmaier, and M. B. Moghadam, *Colloid. Surface. B,* **91**, 280 (2012).
24. Y. L. Lam, C. W. Kan, and C. W. M. Yuen, *Fiber. Polym.*, **11**, 551 (2010).
25. Y. L. Lam, C. W. Kan, C. W. M. Yuen, and C. H. Au, *Fiber. Polym.*, **12**, 626 (2011).
26. K. Kanehira, T. Banzai, C. Ogino, N. Shimizu, Y. Kubota, and S. Sonezaki, *Colloid. Surface. B*, **64**, 102 (2008).
27. A. Fujishima, X. Zhang, and D. A. Turyk, *Surface Science Reports J.*, **63**, 515 (2008).
28. N. Vero, S. Hribernik, P. Andreozzi, and M. S. Smole, *Fiber. Polym.*, **10**, 716 (2009).
29. R. Dastjerdi and M. Montazer, *Colloid. Surface. B*, **88**, 381 (2011).
30. Y. Zhang, Y. Fan, C. Sun, D. Shen, Y. Li, and J. Li, *Colloid. Surface. B*, **40**, 137 (2005).
31. G. Rajagopal, S. Maruthamuthu, S. Mohanan, and N. Palaniswamy, *Colloid. Surface. B*, **51**, 107 (2006).
32. F. Zhang, X. Wu, Y. Chen, and H. Lin, *Fiber. Polym.*, **10**, 496 (2009).
33. R. Dastjerdi, M. Montazer, and S. A. Shahsavan, *Colloid. Surfaces A*, **345**, 202 (2009).
34. T. Jiang, L. Liu, and J. Yao, *Fiber. Polym.*, **12**, 620 (2011).
35. R. Dastjerdi, M. R. M. Mojtahedi, A. M. Shoshtari, A. Khosroshahi, and A. J. Moayed, *Text. Res. J.*, **79**, 1099 (2009).
36. X. Xu and M. Zhou, *Fiber. Polym.*, **9**, 685 (2008).
37. R. Dastjerdi and V. Babaahmadi, *Colloid. Surfaces A*, **386**, 45 (2011).
38. R. Dastjerdi and M. Montazer, *Colloid. Surface. B*, **79**, 5 (2010).